Drug Design, Development and Therapy

Dovepress
open access to scientific and medical research

Open Access Full Text Article

ORIGINAL RESEARCH

A Novel Network Pharmacology Strategy Based on the Universal Effectiveness-Common Mechanism of Medical Herbs Uncovers Therapeutic Targets in Traumatic Brain Injury

Zhe Yu[1–3], Ruoqi Ding[1–3], Qiuju Yan[1–3], Menghan Cheng[1–3], Teng Li[1–4], Fei Zheng[5], Lin Zhu[1–4], Yang Wang[1–4], Tao Tang[1–4], En Hu[1–4]

[1]Institute of Integrative Medicine, Department of Integrated Traditional Chinese and Western Medicine, Xiangya Hospital, Central South University, Changsha, 410008, People's Republic of China; [2]NATCM Key Laboratory of TCM Gan, Xiangya Hospital, Central South University, Changsha, 410008, People's Republic of China; [3]Center for Interdisciplinary Research in Traditional Chinese Medicine, Xiangya Hospital, Central South University, Changsha, 410008, People's Republic of China; [4]Xiangya Hospital, Central South University, Nanchang, Jiangxi, 330004, People's Republic of China; [5]The College of Integrated Traditional Chinese and Western Medicine, Hunan University of Chinese Medicine, Changsha, 410008, People's Republic of China

Correspondence: En Hu; Ruoqi Ding, Integrative Medicine, Department of Integrated Traditional Chinese and Western Medicine, Xiangya Hospital, Central South University, Changsha, 410008, People's Republic of China, Email znxyhe@csu.edu.cn; ruoqi_ding@outlook.com

Purpose: Many herbs can promote neurological recovery following traumatic brain injury (TBI). There must lie a shared mechanism behind the common effectiveness. We aimed to explore the key therapeutic targets for TBI based on the common effectiveness of the medicinal plants.

Material and methods: The TBI-effective herbs were retrieved from the literature as imputes of network pharmacology. Then, the active ingredients in at least two herbs were screened out as common components. The hub targets of all active compounds were identified through Cytohubba. Next, AutoDock vina was used to rank the common compound-hub target interactions by molecular docking. A highly scored compound-target pair was selected for in vivo validation.

Results: We enrolled sixteen TBI-effective medicinal herbs and screened out twenty-one common compounds, such as luteolin. Ten hub targets were recognized according to the topology of the protein-protein interaction network of targets, including epidermal growth factor receptor (EGFR). Molecular docking analysis suggested that luteolin could bind strongly to the active pocket of EGFR. Administration of luteolin or the selective EGFR inhibitor AZD3759 to TBI mice promoted the recovery of body weight and neurological function, reduced astrocyte activation and EGFR expression, decreased chondroitin sulfate proteoglycans deposition, and upregulated GAP43 levels in the cortex. The effects were similar to those when treated with the selective EGFR inhibitor.

Conclusion: The common effectiveness-based, common target screening strategy suggests that inhibition of EGFR can be an effective therapy for TBI. This strategy can be applied to discover core targets and therapeutic compounds in other diseases.

Keywords: traditional Chinese medicine, medicinal plants, luteolin, AZD3759, epidermal growth factor receptor, astrocyte

Introduction

Traumatic brain injury (TBI) is a major cause of morbidity, mortality, and disability worldwide. It costs approximately $400 billion annually worldwide. However, no FDA-approved drugs are available for post-TBI improvement. Therefore, it is urgent to develop new therapies for TBI.[1]

Various herbs have shown shared therapeutic effects in experimental studies of TBI. They can improve mNSS scores, reduce brain water content, and decrease neuron loss.[2] One of the possible reasons these different herbs can exert the same therapeutic effect on TBI is that they may target shared pathological mechanisms[3,4]. For example, *Crocus sativus L*. protects the post-TBI brain from inflammatory and oxidative injury,[5] and *Panax notoginseng* inhibits autophagy to rescue brain damage.[6] These

Received: 5 December 2023
Accepted: 10 April 2024
Published: 16 April 2024

medicinal plants usually exert their therapeutic effects through a multiple-component and multiple-target approach.[7] Thus, we speculated that the common therapeutic effects may originate from their shared active compounds and common targets. Uncovering the shared targets and targets of these medicinal herbs will help find the core target and therapeutic ingredients for TBI. This effectiveness-directed target-discovery method can be an alternative to traditional pathophysiology-based strategies. Moreover, to a certain extent, the new approach can be more efficient due to the validated effectiveness of the imputed herbs.

Network pharmacology is a systematic bioinformatics method extensively utilized to investigate the potential mechanisms of herbal medicines in diseases.[8,9] It screens active compounds, predicts compound targets, intersects targets of compounds and diseases, and then constructs a comprehensive herb-component-targets-disease network. By integrating molecular docking and experimental validation, network pharmacology has discovered the active ingredients and targets of herbs in diseases, including TBI.[10–12] It may be an effective tool to explore the common compounds and targets of different herbs.

This work aimed to identify the core targets of TBI based on the common effectiveness and mechanism of different TBI-treating herbs. First, we screened the shared compound-core target interactions by network pharmacology and molecular docking. Then, the therapeutic potential of a core target was validated by administering the corresponding herbal compound and a selective inhibitor to TBI mice (Figure 1).

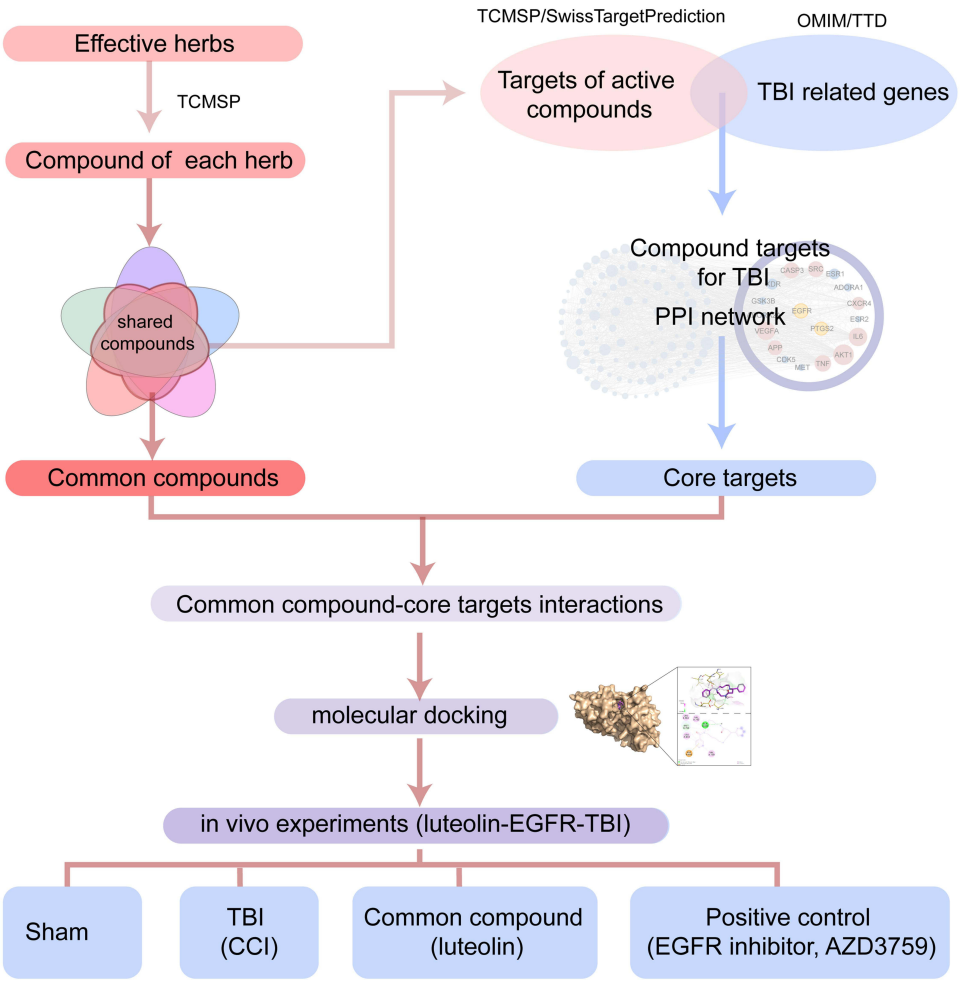

Figure 1 Flowchart of this research. The common compounds of the effective herbs and the compound targets in TBI are screened. The potential common compounds-core target interactions are assessed by molecular docking and in vivo experiments.

Materials and Methods

Enrollment of the TBI-Effective Medicinal Plants

The TBI-treating medicinal plants were searched from PubMed, Medline, and Scopus (1976 to November 2020). Reviews, editorials, and origin articles were collected. The search terms included "medicinal plants", "traumatic brain injury", "fluid percussion injury", "cortical impact injury (CCI)", "lateral fluid percussion", "weight drop–impact acceleration injury (WDIAI)", and "blast injury". The resulting publications were then screened manually to exclude irrelevant publications, and the herbal formula consisted of more than one medicinal plant.

Network Pharmacology-Based Common Compound and Core Target Prediction

All chemical compounds of the 16 medicinal plants were collected from the Traditional Chinese Medicine Systems Pharmacology (TCMSP) Database (http://lsp.nwsuaf.edu.cn/tcmsp.php). The candidate compounds were screened according to the criteria of drug-likeness (DL) ≥ 0.18 and oral bioavailability (O.B.) ≥ 30%.[13] The potential targets of compounds were obtained from the TCMSP and SwissTargetPrediction (http://swisstargetprediction.ch/) databases. Then, the TBI-associated targets were gathered from OMIM (https://www.omim.org/) and TTD (http://bidd.nus.edu.sg/group/cjttd/). Finally, the overlapping genes between plant- and TBI-associated targets were identified as the potential targets of the 16 medicinal plants against TBI.

Protein-Protein Interaction (PPI) Network and Analysis

The overlapping genes were input into the STRING database (https://string-db.org/) to quantify their interactions (confidence score > 0.900). Then, Cytoscape software (version 3.7.2) was used to visualize the topological properties of the PPI network. Furthermore, CytoHubba was processed to analyze the core nodes in the PPI network.[14]

Molecular Docking

The epidermal growth factor receptor (EGFR) crystal structure was acquired from the RCSB Protein Data Bank (https://www.rcsb.org/, PDB_ID: 5UG9). Ligand files of active compounds were downloaded from PubChem (https://pubchem.ncbi.nlm.nih.gov/, PubChem_ID shows in Table S1). The structure of MOL002927 was the same as that of MOL002934 in PubChem. AutoDockTools 1.5.6 was used to convert target and ligands to pdbqt formats. Then, water was deleted, and hydrogen atoms were added. The active pocket of EGFR was coordinated at center_x = −3.747, size_x = 40, center_y = 19.028, size_y = 40, center_z = −21.393, and size_z = 40. Molecular docking was carried out using AutoDock Vina (Version 1.1.2), with an energy range of four and an exhaustiveness of 8. Finally, the molecular conformations with relatively high affinity were visualized along with their corresponding targets by PyMOL (version 2.2.0) and Discovery Studio visualizer (version 4.5).

Animals

Eight-week-old C57BL/6 male mice were obtained from Hunan Slake Jingda Laboratory Animal Co., Ltd. All mice were housed in a well-ventilated room at 25°C with a 12 h dark-light cycle. Mice received free access to food and water. Animal care was performed according to the NIH Guide for the Care and Use of Laboratory Animals (NIH Publication No. 80–23; revised 1978). The animal protocols were approved by the Committee on the Use and Care of Animals of Central South University (CSU-2022-0001-0035).

Experimental Groups and TBI Induction

TBI experiments were performed using the controlled cortical impact (CCI) model as described.[10,12] The CCI was produced with a pneumatically driven PSI TBI-0310 Impactor (Precision Systems & Instrumentation LLC, Fairfax, VA, USA). The parameters were set as follows: impact depth, 1 mm; striking speed, 3.5 m/s; dwell time, 80 ms. The mice in the sham group underwent the same surgery as CCI animals, except for cortical impact.

Experimental Design

Sample size of animals was determined using sample size calculator (http://www.lasec.cuhk.edu.hk/sample-size-calculation.html), on condition that $\alpha = 0.05$, $1\text{-}\beta = 0.9$, the 14-day mNSS of CCI mice is 5.5 ± 0.8, while the treated group scores 3.8 ± 0.8. As a result, 6 mice were used in each group.

Animals were randomly divided into five groups: sham, TBI, TBI + AZD3795 (a selective BBB penetrating EGFR inhibitor, #S7971, Selleck Shanghai China, 15 mg/kg), TBI + luteolin 50 mg/kg, and TBI + luteolin 25 mg/kg. AZD3759 was dissolved in 0.5% sodium carboxymethyl cellulose (CMC-Na, #S6703, Selleck Shanghai, China). Mice in other groups were intragastrically treated with an equal volume of 0.5% CMC-Na solution daily. The doses of AZD3759 were based on a previous study.[15] Luteolin (B20888, purity > 98%, Shanghai Yuanye Bio-Technology Co., Ltd, Shanghai, China) was dissolved in the solution, including 1% dimethyl sulfoxide (DMSO), 40% polyethylene glycol (PEG) 300, 5% Tween 80, and 64% saline. Luteolin or an equal volume of solvent was injected intraperitoneally daily for 14 days. No mice died until sampling.

Hematoxylin and Eosin (H&E) Staining and Nissl Staining

For H&E staining, paraffin sections were deparaffinized, rehydrated, and stained in hematoxylin solution (G1004, Servicebio, Wuhan, China) for 5 min and eosin solution (G1001, Servicebio) for 15 sec. For Nissl staining, the hydrated sections were stained with toluidine blue solution (G1036, Servicebio) for 8 min. Following staining, slices were dehydrated, hyalinized, and mounted.

Immunofluorescence

For immunofluorescence, antigens were retrieved by boiling sections in citrate buffer (pH 6.0) for 20 minutes. After being blocked with 3% bovine serum albumin (#9048-46-8, Genview Inc., Shanghai, China), the slices were incubated overnight at 4°C with the following primary antibodies: mouse anti- glial fibrillary acidic protein (GFAP) (1:1500, #SC33673, Santa Cruz), rabbit anti- growth associated protein 43 (GAP43) (1:800, #8945, Cell Signaling Technology), rabbit anti-EGFR (1:200, #4267, Cell Signaling Technology), and rabbit anti-Brevican (1:30, ab285162, Abcam, Cambridge, MA, USA). Secondary antibodies included AlexaFluor-488-conjugated secondary antibody (1:1000, Jackson ImmunoResearch, West Grove, PA, USA) and Cy3-conjugated secondary antibody (1:1000, Jackson ImmunoResearch). The secondary antibody was incubated for 1 hour at room temperature.

Statistical Analysis

The data are expressed as the mean ± standard error (SEM). QQ plots were utilized to assess data distribution. Data conforming to normal distribution were compared using Welch- ANOVA followed by a Dunnett's T3 multiple comparisons test, while those with non-normally distributed were tested using Kruskal-Wallis followed by Dunn's multiple comparisons. For data with sample size below five, bootstrapping (100 iterations, by R 4.2.1, boot package) was used to calculate the means and corresponding 95% confident intervals. A value of $P < 0.05$ was considered statistically significant.

Results

The Common Targets of the TBI Effective Medical Plants

First, sixteen medicinal plants were collected from the literature, including *Achyranthis Bidentatae Radix* (*A. Bidentatae), Artemisia annua* (*A. Annua), Carthamus tinctorius* (*C. Tinctorius), Centella asiatica* (*C. Asiatica), Cnidium monnieri* (*C. Monnieri), Crocus sativus* (*C. Sativus), Curcuma longa* (*C. Longa), Curcuma zedoaria* (*C. Zedoaria), Drynaria fortune* (*D. Fortune), Erigeron breviscapus* (*E. Breviscapus), Forsythia suspensa* (*F. Suspensa), Panax ginseng* (*P. Ginseng), Polygonum cuspidatum* (*P. Cuspidatum), Rheum tanguticum* (*R. Tanguticum), Salvia miltiorrhiza* (*S. Miltiorrhiza*), and *Scutellaria baicalensis* (*S. Baicalensis*). Then, 230 compounds were screened from the TCMSP database based on the O.B. and DL. These candidate compounds include 65 in *S. Miltiorrhiza*, 24 in *S. Baicalensis*, 23 in *F. Suspensa*, 22 in *A. Annua*, 22 in *C. Tinctorius*, 22 in *P. Ginseng*, 20 in *A. Bidentatae*, 19 in *C. Monnieri*, 18 in

D. Fortune, 16 in *R. Tanguticum*, 12 in *E. Breviscapus*, 10 in *P. Cuspidatum*, 5 in *C. Sativus*, 3 in *C. Asiatica*, 3 in *C. Longa*, and 3 in *C. Zedoaria*, respectively (Table S2). Next, a medicinal plant-candidate compound network (Mp-Cc network) was built (Figure 2). In this network, compounds present in more than one herb were identified as common compounds. As a result, there were 21 common compounds and 209 unique compounds. The common compounds included beta-sitosterol, luteolin, quercetin, kaempferol, and stigmasterol (Table 1).

The Core Targets of TBI-Treating Medical Plants in TBI

To display the relationship between the herbal compounds and their targets, we established a Cc-candidate target (Ct) network (Figure S1). In this network, 1177 targets and 230 compounds formed 21,564 interactions. Details of the top target proteins are shown in Table S3. Since the 16 medicinal plants have shown effectiveness in treating TBI, we analyzed the PPI network of all targets of these medicinal plants. The top 10 hub genes in this network were AR, CDK2, ESR2, ESR1, GSK3B, CYP19A1, KDR, EGFR, PTGS2, and ACHE (Figure S2A and Table S3). The targets were mostly enriched in neurovascular regeneration (BDNF signaling pathway, VEGFA-VEGFR2 signaling pathway) and cell migration (Focal adhesion, PI3K-Akt signaling pathway) (Figure S2B–E).

To explore the potential targets of the medicinal plants in treating TBI, we gathered the TBI-related genes in the OMIM and TTD databases and intersected them with the targets of herbal compounds. As a result, 131 overlaps were obtained from the 585 TBI-related targets (Figure 3A). Then, we constructed the PPI network of the overlapping targets and analyzed the topology by CytoHubba (Figure 3B). As evaluated by the integrated scores of 10 computational methods in Cytohubba, the top 10 genes were considered hub genes, including VEGFA, IL6, SRC, TNF, CASP3, APP, AKT1, CXCR4, PTGS2, and EGFR (Table 2). Detailed information on the ranking of the 10 computational methods is

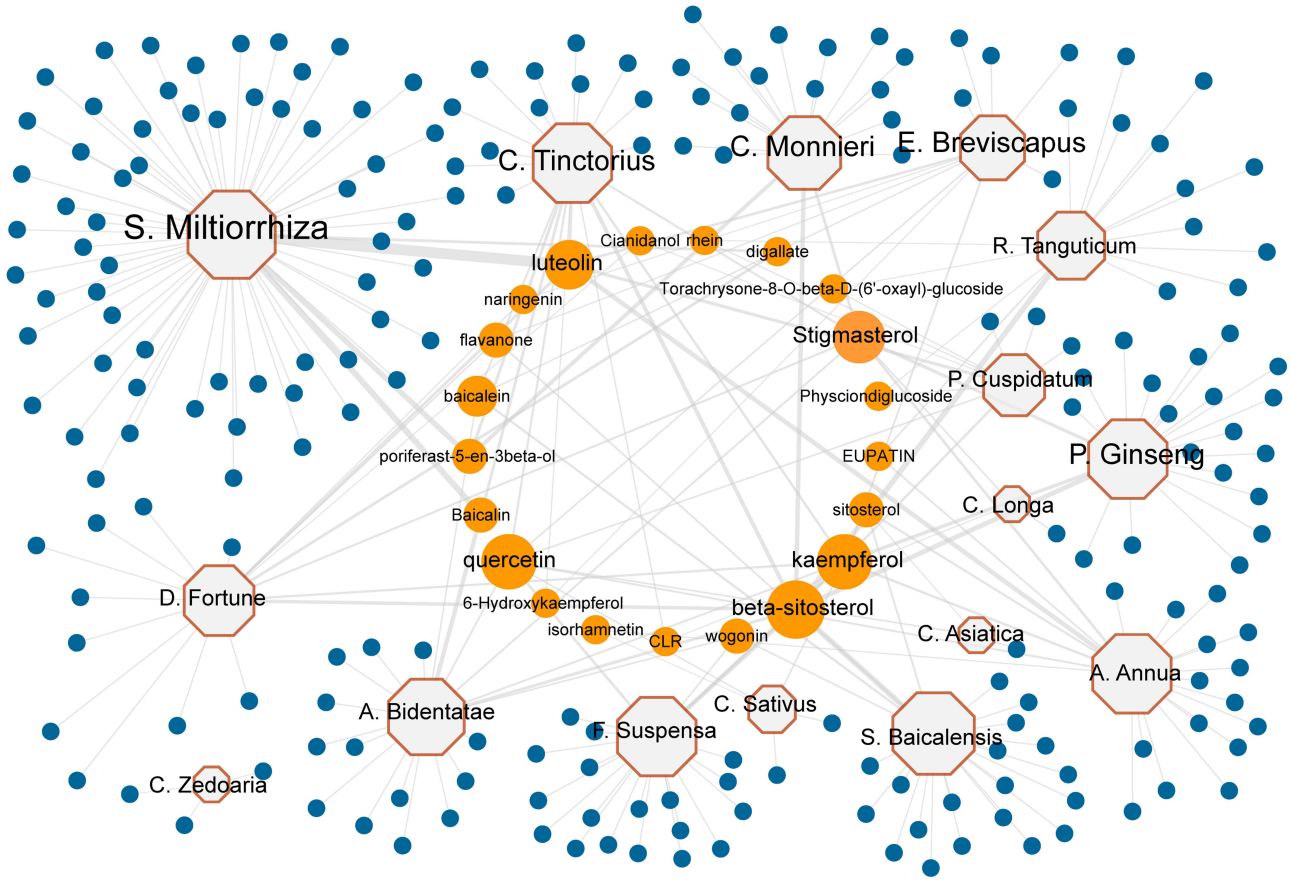

Figure 2 The herb-compound network of the collected effective herbs. Sixteen TBI-effective herbs consist of 230 compounds. Octagons represent medicinal plants. Circles represent candidate compounds. Blue circles represent 209 specific compounds, and Orange circles represent 21 common compounds. The size of the node is proportional to the value of degree.

Table 1 The Information About the Shared Compound

Compound	Source Number	Source	OB (%)	DL
Beta-sitosterol	9	*A. Annua, C. Monnieri, C. Tinctorius, D. Fortune, F. Suspensa, P. Cuspidatum, P. Ginseng, P. Ginseng, S. Baicalensis*	36.91	0.75
Luteolin	7	*A. Annua, C. Tinctorius, D. Fortune, E. Breviscapus, F. Suspensa, P. Cuspidatum, S. Miltiorrhiza*	36.16	0.25
Kaempferol	7	*A. Annua, C. Sativus, C. Tinctorius, D. Fortune, E. Breviscapus, F. Suspensa, P. Ginseng*	41.88	0.24
Quercetin	7	*A. Annua, C. Asiatica, C. Sativus, C. Tinctorius, E. Breviscapus, F. Suspensa, P. Cuspidatum*	46.43	0.28
Stigmasterol	6	*A. Annua, C. Longa, C. Monnieri, C. Tinctorius, D. Fortune, P. Ginseng*	43.83	0.76
Baicalein	4	*A. Annua, C. Tinctorius, E. Breviscapus, S. Baicalensis*	33.52	0.21
Baicalin	3	*A. Annua, C. Tinctorius, S. Miltiorrhiza*	40.12	0.75
Eriodyctiol (flavanone)	3	*D. Fortune, E. Breviscapus, S. Baicalensis*	41.35	0.24
Poriferast-5-en-3beta-ol	3	*C. Monnieri, C. Tinctorius, S. Miltiorrhiza*	36.91	0.75
Sitosterol	3	*A. Annua, C. Asiatica, S. Baicalensis,*	36.91	0.75
Wogonin	3	*A. Annua, F. Suspensa, S. Baicalensis*	30.68	0.23
(+)-catechin	2	*D. Fortune, P. Cuspidatum*	54.83	0.24
(2R)-5,7-dihydroxy-2-(4-hydroxyphenyl) chroman-4-one	2	*D. Fortune, E. Breviscapus*	42.36	0.21
6-Hydroxykaempferol	2	*C. Tinctorius, E. Breviscapus*	62.13	0.27
CLR	2	*C. Longa, C. Tinctorius*	37.87	0.68
Digallate	2	*D. Fortune, S. Miltiorrhiza*	61.85	0.26
Eupatin	2	*A. Annua, P. Ginseng*	50.80	0.41
Isorhamnetin	2	*A. Annua, C. Sativus*	49.60	0.31
Physciondiglucoside	2	*P. Cuspidatum, P. Ginseng*	41.65	0.63
Rhein	2	*P. Cuspidatum, P. Ginseng,*	47.07	0.28

Abbreviations: OB, oral bioavailability; DL, drug likeness.

shown in Table S4. In addition, the pathways enriched with the targets were mainly related to the AGE/RAGE pathway and EGFR tyrosine kinase inhibitor resistance pathway (Figure 3C). According to the results of the topological analyses of the two PPI networks and the pathway enrichment analysis, EGFR can be one of the core targets in TBI.

Molecular Docking Validation of the Compound-Core Target Interaction

In the Cc-Ct network, EGFR interacted with 77 herbal compounds. To further investigate the possibility of interaction between EGFR and active components, we applied molecular docking studies (Table S5). By comparing docking scores, the top three active ingredients were celabenzine, luteolin, and baicalin (Table S5, Figure 3D, Figure S3A and B). Because celabenzine was commercially unavailable, we assessed the luteolin-EGFR interaction in the following experiments. As shown in Figure 3D, luteolin formed a pi-sigma bond with MET-766, two hydrogen bonds with ASP-855 and CYS-775, and three pi-alkyl bonds with VAL-769, ALA-859, and LEU-833 (Figure 3D). In addition, the brain RNA-Seq database (https://brainrnaseq.org/) indicated that EGFR is primarily located on astrocytes in both *Homo sapiens* and *Mus musculus* (Figure S3C and D). Moreover, AZD03759, a known inhibitor of EGFR, docked to a similar pocket in EGFR to luteolin (docking score: −8.6), (Figure S3E).

The Effects of Luteolin and AZD3759 on Post-TBI Recovery

The mNSS showed that the scores of CCI mice were significantly higher than those of the sham group after surgery (day 0), indicating the successful establishment of the model. There was no significant difference between the luteolin and CCI groups on days 0, 1, and 3 (Figure S4A). Notable differences in the AZD3759 and luteolin 50 mg/kg groups compared to the CCI group were observed on day 7 and day 14 (Figure 4B).

The foot fault rate of the CCI group was significantly elevated compared with that of the luteolin group on day 14 but not on days 1, 3, and 7 (Figure 4C and Figure S4B). The initial body weights were not significantly different among the five groups (Figure S4C). However, marked differences in the AZD3759, luteolin 50 mg/kg, and luteolin 25 mg/kg groups compared to the CCI group were observed on day 14 (Figure 4D).

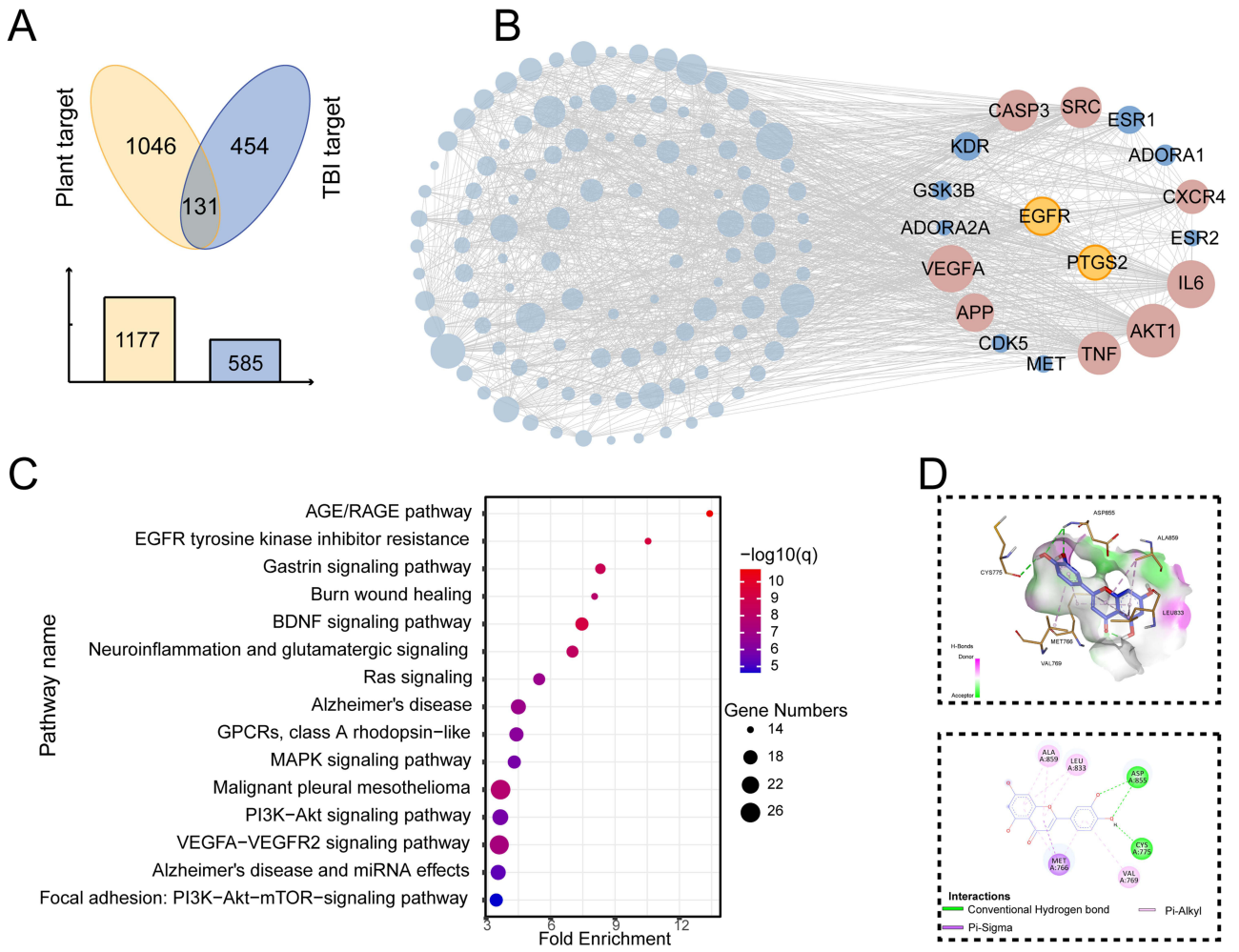

Figure 3 The common compound-core target interactions. (**A**) Venn diagram shows 131 overlapped genes between herb targets and TBI-related genes. (**B**) The PPI network of the overlapping targets highlights the core targets of TBI, including EGFR. (**C**) The top 15 enriched Wiki pathway of the overlapped targets shows the importance of the AGE/RAGE pathway, and EGFR tyrosine kinase inhibitor resistance pathways in TBI. (**D**) The 3D and 2D interaction diagrams display the binding model of luteolin and EGFR.

H&E staining of ipsilateral injured brain cortices on day 14 showed infiltration of inflammatory cells, neuronal necrosis, karyolysis and vacuolar changes, and enlarged intercellular gaps in the CCI group. AZD3759 treatment and luteolin treatment reduced these anomalies (Figure 4A).

Table 2 The Rank Summary of the Top 10 Central Targets in the PPI Network of the TBI-Related Compound Targets

Targets	MCC	MNC	Degree	EPC	BottleNeck	EcCentricity	Closeness	Radiality	Betweenness	Stress	Rank sum
VEGFA	4	3	3	2	1	2	3	3	4	3	1
IL6	5	2	2	3	4	5	2	2	2	2	2
SRC	7	6	6	5	2	3	6	6	3	4	3
TNF	6	4	4	4	3	4	4	4	8	8	4
CASP3	3	5	5	6	5	6	5	5	6	7	5
APP	20	8	8	11	8	1	7	7	5	5	6
AKT1	17	1	1	1	36	33	1	1	1	1	7
PTGS2	13	10	10	9	6	7	10	10	15	13	8
CXCR4	1	12	12	10	15	14	12	12	19	15	9
EGFR	8	7	7	7	37	34	8	8	9	9	10

Abbreviations: MCC, Maximal Clique Centrality; MNC, Maximum Neighborhood Component; EPC, Edge Percolated Component.

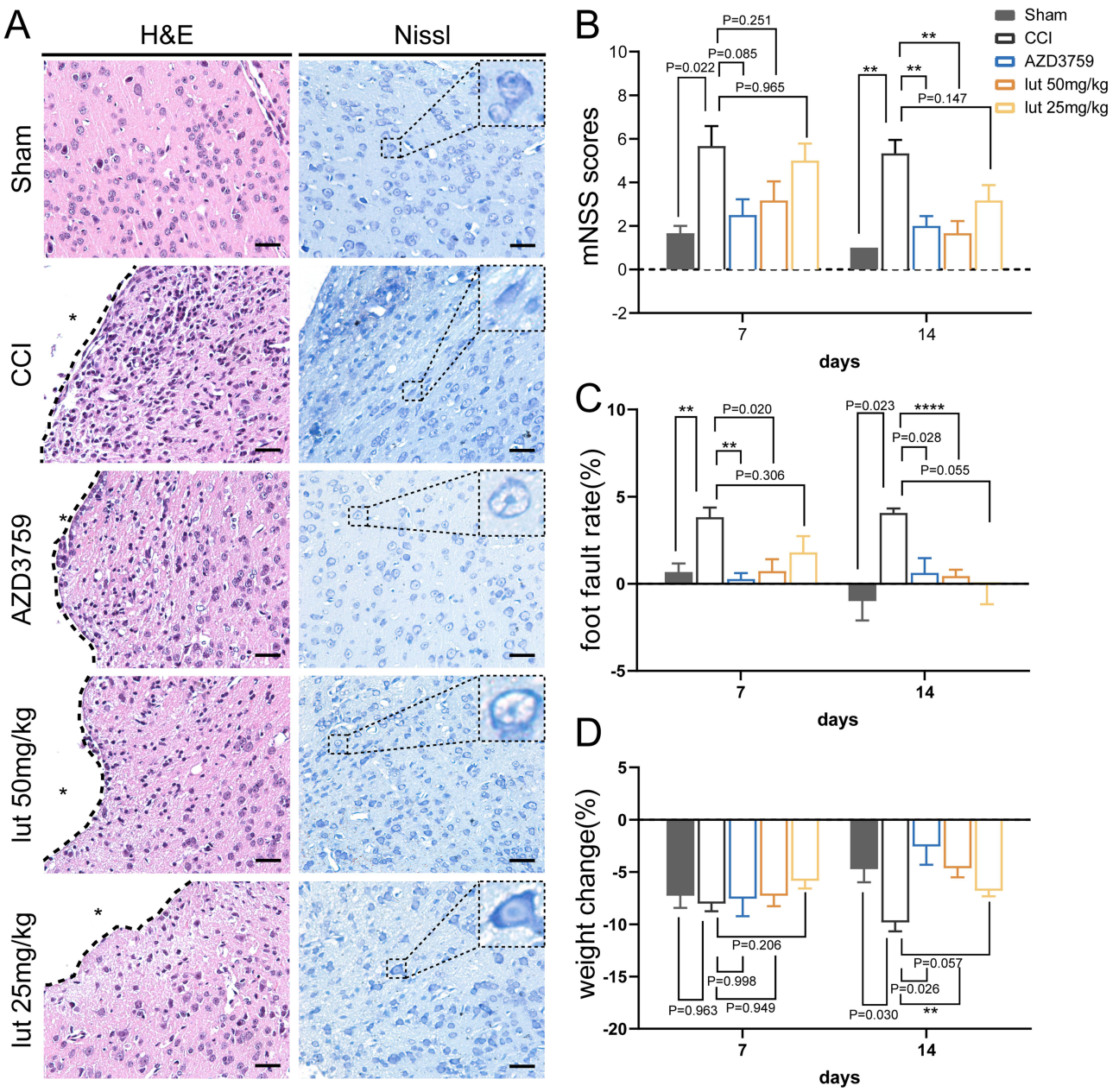

Figure 4 The therapeutic effects of luteolin in treating CCI mice. (**A**) H&E staining and Nissl staining of the cerebral cortex (N=3). The dotted lines indicate the damaged region. (**B**) mNSS shows that AZD3759 and luteolin partially reverse the neurological deficits of the CCI mice on days 7 and 14. (**C**) Foot fault test suggests that AZD3759 and luteolin reduce the foot fault rate after CCI. (**D**) AZD3759 and luteolin alleviate the body weight loss after CCI. Data are expressed as Mean ± SEM, N = 6 (**B-D**), $^{**}P < 0.01$, $^{****}P < 0.0001$, Scar bar = 100 μm. CCI: Controlled Cortical Impact model.

Nissl staining shows surviving neurons in the cortex in each group. As shown in Figure 4A, the Nissl bodies in the CCI group were blurred and pyknotic nuclei. The cells were small with an insufficient cytoplasm and blurred nucleoli. In the AZD3759- and luteolin-treated groups, abnormal Nissl bodies were reduced.

The Effects of Luteolin and AZD3759 on EGFR and Astroglia Scar Formation After TBI

According to the results of mouse brain RNA sequencing,[16] EGFR is mainly expressed in astrocytes (Figure S3C and D). To determine whether the expression of EGFR was augmented in astrocytes when the brain nerve was injured, we performed double-labeling immunofluorescence for EGFR and GFAP after CCI (Figure 5A). Few colocalizations of EGFR and GFAP

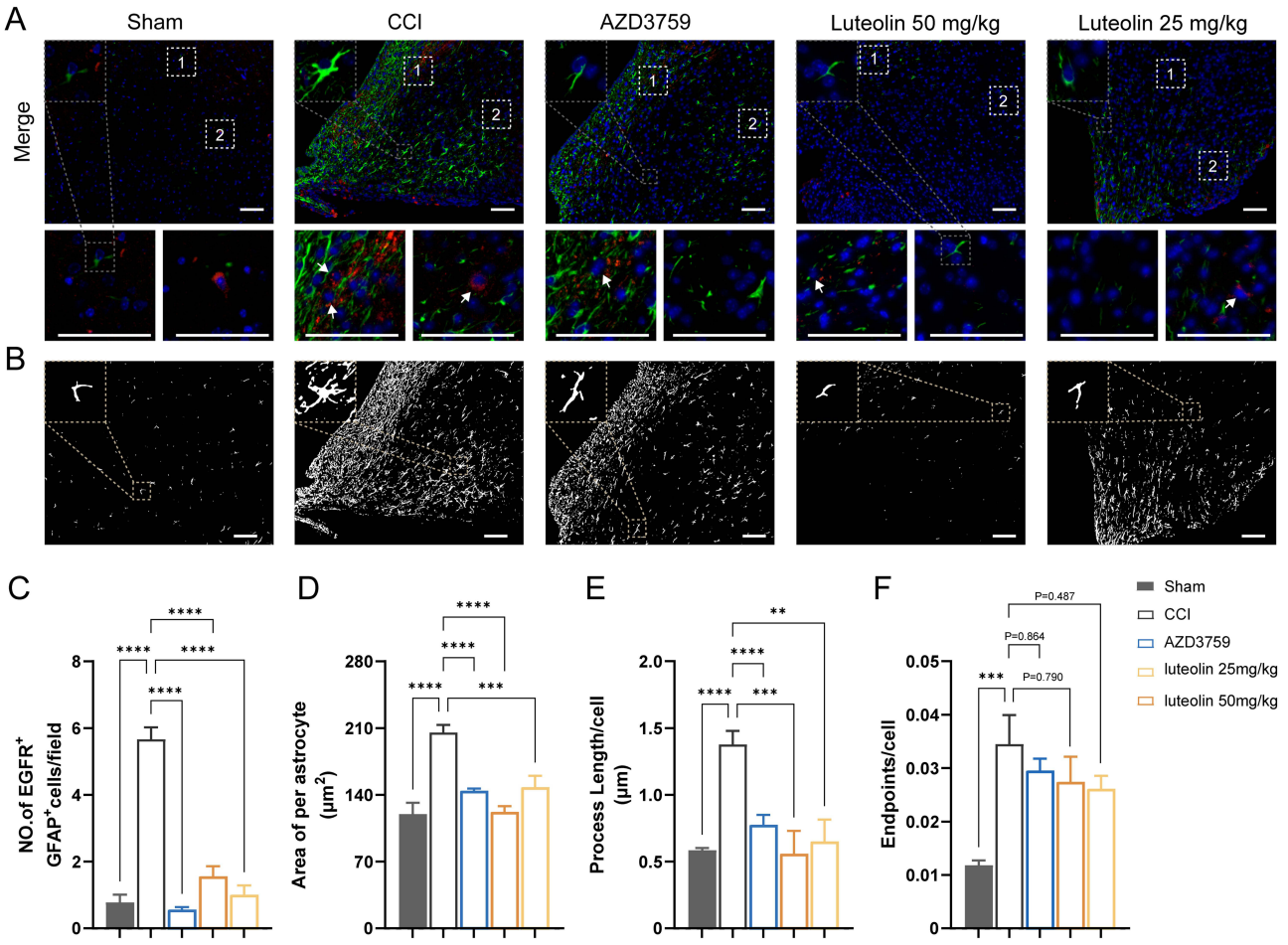

Figure 5 Luteolin and AZD03759 attenuate astrocyte activation after CCI. (**A**) Immunofluorescent staining of GFAP (green) and EGFR (red) shows luteolin and AZD03759 decrease astrocyte number and astrocytic EGFR expression. (**B**) Morphological analysis suggests luteolin and AZD03759 suppress astrocyte activation. (**C**) Quantification of both EGFR-positive and GFAP-positive cells. (**D-F**) Quantitative metrics of astrocyte activation. Data are expressed as Mean ± SEM, N = 3, $^{**}P < 0.01$, $^{***}P < 0.001$, $^{****}P < 0.0001$, Scar bar = 50 μm. CCI: Controlled Cortical Impact model.

were observed from the mouse cerebral cortex in the sham group. However, in the CCI group, the number of $EGFR^+/GFAP^+$ cells surrounding the damaged area increased. Administration of an inhibitor of EGFR tyrosine kinase, AZD3759, not only significantly reduced EGFR immunoreactivity in astrocytes but also suppressed GFAP expression after CCI. In the luteolin group, the number of EGFR and GFAP double-positive cells was decreased (Figure 5A–C). In addition, luteolin decreased the swollen volume and process length of astrocytes after CCI (Figure 5B, D and E). Moreover, luteolin and AZD3759 tended to reduce the number of astrocyte endpoints (Figure 5F). In conclusion, luteolin and AZD3759 suppressed EGFR expression and astrocyte activation after CCI.

Reactive astrocytes, together with their product CSPGs, form glial scars, which hamper axon regeneration in the peri-injured area of the brain. To explore the effect of EGFR and on glial scar formation and axon regeneration, we performed immunofluorescence staining of brevican (a kind of GSPG), GFAP and GAP43. We found higher expression of brevican in the damaged region of the CCI group than in the other group (Figure 6A and B). Moreover, immunofluorescence staining of GFAP suggested that the average scar area and maximal scar area of the cortex decreased in the luteolin group and AZD3759 group compared with the CCI group (Figure 6C and D). Therefore, luteolin could attenuate glial scar formation by reducing astrocyte activation after CCI.

Additionally, there was a small amount of GAP43 expression around the injured cortex in the sham and CCI mice. After luteolin treatment, the expression of GAP43 was elevated, similar to that in the AZD3759-treated group. This result suggested that luteolin and AZD3795 facilitated post-TBI axonal regeneration (Figure 7).

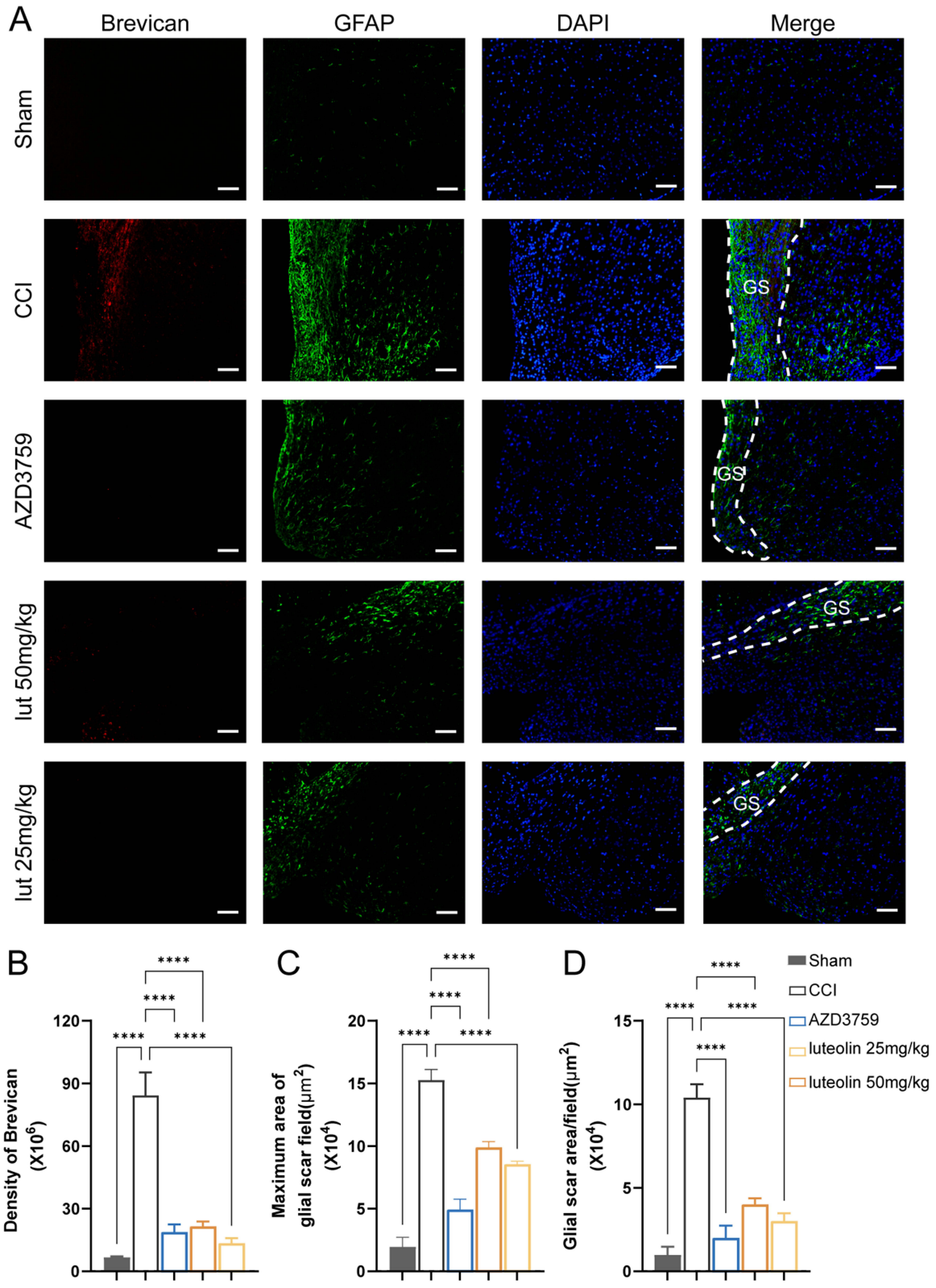

Figure 6 Luteolin reduced glial scar formation after CCI. (**A**) Immunofluorescent staining of GFAP (green) and Brevican (red, CSPGs marker). (**B**) Quantification of Brevican expression. (**C**) The maximum area of the glial scar. (**D**) The average glial scar area. Data are expressed as Mean ± SEM, N = 3, ****$P < 0.0001$, Scar bar = 50 μm. CCI: Controlled Cortical Impact model.

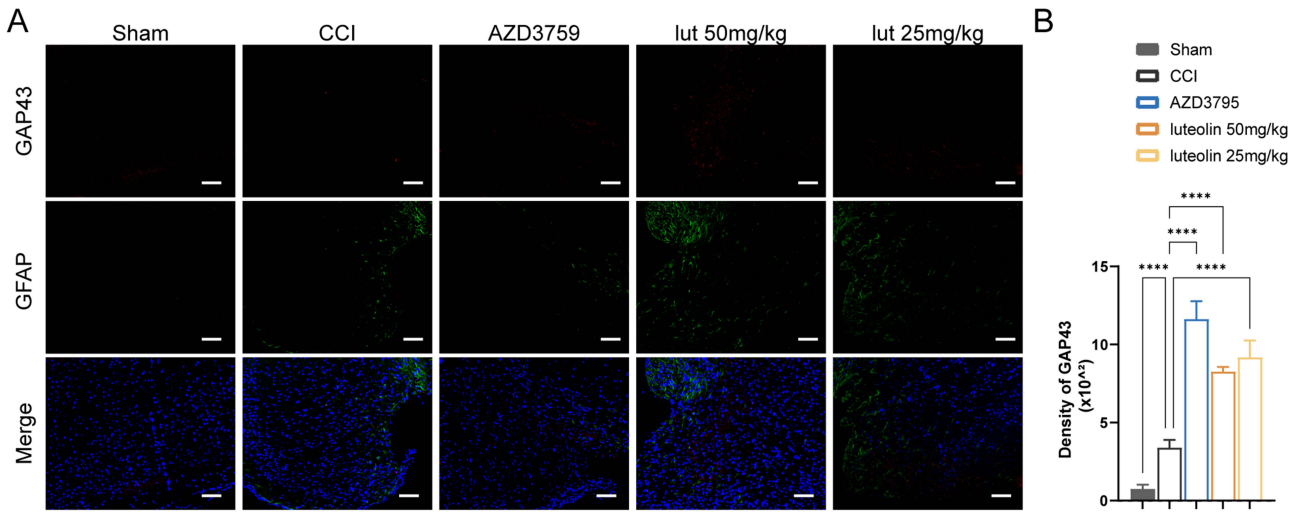

Figure 7 Luteolin promoted axonal regeneration after CCI. (**A**) Immunofluorescent staining of GFAP (green) and GAP43 (red). (**B**) Quantification of GAP43 expression. Data are expressed as Mean ± SEM, N = 3, ****$P < 0.0001$, Scar bar = 50 μm. CCI: Controlled Cortical Impact model.

Discussion

In the present study, we developed a common efficacy and common mechanism-based network pharmacology strategy to explore the core target and relevant therapeutic compound in TBI. The strategy found twenty-one compounds as potential common compounds among sixteen neuroprotective herbs in TBI. It also highlighted ten hub proteins as candidate core targets for TBI, including EGFR. Molecular docking calculations showed that luteolin firmly bound to EGFR. Moreover, in vivo experiments validated that luteolin and the selective EGFR inhibitor AZD3759 suppressed astrocyte activation and glial scar formation, facilitated axon sprouting, and promoted neurological recovery after TBI. This study is the first to report that EGFR is a promising target for post-TBI improvement and that luteolin and AZD3759 may be candidate EGFR inhibitors for treating TBI. This novel strategy may be applied in other diseases to explore the core therapeutic targets.

EGFR is a member of the receptor tyrosine kinase superfamily.[17] EGFR signaling is essential for the development of astrocytes and neurons in the developing central nervous system, but upon differentiation in the adult central nervous system, EGFR expression in these cells is reduced, and its activation is absent in the adult brain.[18] Upon spinal cord injury, EGFR increases, especially in reactive astrocytes.[19] Our results confirm that astrocytic EGFR is elevated around the injured cortex after TBI. EGFR activation promotes astrocyte activation and secretion of CSGPs to form glial scars, which hamper axonal sprouting after injury.[20–23] In our present research, astrocyte activation and CSGPs expression were positively correlated with EGFR expression, which was consistent with a previous study.[24] Studies have also shown that pharmacological blockade of EGFR activation and astrocytic scar formation improves axonal regrowth and better functional outcomes in spinal cord injury.[20–22,25] This finding agrees with our findings in TBI, suggesting that inhibition of EGFR reduces astrocytic scar formation and promotes axonal regeneration and functional recovery in TBI. The results imply that EGFR can be a promising therapeutic target for TBI.

AZD3759, also called zorifertinib, is the first selective EGFR antagonist.[26] Long-term dosing of AZD3759 shows no apparent toxicity in phase I studies.[26,27] Moreover, it can permeate the blood–brain barrier (BBB).[26,28] Therefore, it can inhibit brain glioma in animal experiments.[29] Additionally, a study reported that AZD3759 attenuates α-synuclein pathology in a mouse model of Parkinson's disease.[26] The docking results implies that AZD3759 binds to the similar active pocket of EGFR to luteolin with slightly stronger affinity. Thus, we chose AZD3759 as a positive tool. The in vivo results validated the therapeutic potential of EGFR inhibition in TBI. Moreover, we noticed superior efficacy of AZD3759 than luteolin for some parameters, which suggests that AZD3759 may also be a potential drug to treat TBI.

Luteolin is an active compound in many herbs, including C. Tinctorius, E. Breviscapus, and P. Cuspidatum.[30–32] It can freely penetrate the BBB.[3,13] In the current study, we calculated that luteolin can bind to EGFR firmly by AutoDock

Vina. It consists of another study predicting interactions via Discovery Studio.[33] To assess the effects of the luteolin-EGFR interaction, we injected luteolin into TBI mice intraperitoneally as previously reported.[13] We suggest that luteolin can reduce EGFR and downstream scar formation in the subacute stage of TBI. The neuroprotective effects of luteolin on TBI animals are supported by an earlier study.[13] However, this study indicates that the neuroprotective effect of luteolin in the acute stage of TBI is Nrf2-ARE dependent.[13] It seems that luteolin has multiple targets, EGFR and Nrf2. The discrepancy in the main targets between the two studies may come from the different pathological states regarding the stages of TBI. In the acute phase, oxidative stress bursts, and the antioxidative nuclear factor Nrf2 is upregulated.[4] EGFR is also enhanced in this stage.[34] However, the astrocytic scar has not formed. Therefore, the neuroprotective effects of luteolin can be blocked by Nrf2 depletion.[13] In the subacute stage, oxidative stress fades, followed by Nrf2 reduction. The glial scar is thickened to form a barrier that hampers axonal regeneration.[35] Thus, the effect of luteolin on EGFR and glial scars is more prominent.

There are several limitations in our study. First, the efficacy of the new strategy needs to be validated in other diseases. Second, candidate core targets other than EGFR should be tested in future studies. Third, the effect of other predicted high-affinity inhibitors of EGFR, such as celabenzine and baicalin, on TBI remains elusive.

Conclusion

For the first time, we developed a strategy to explore the targets of disease by investigating the common mechanisms of medicinal plants based on their common effectiveness. We identified EGFR as a core therapeutic target and luteolin and AZD3759 as candidate therapeutic drugs in TBI. We also suggest that luteolin can bind EGFR to reduce EGFR-mediated glial scar formation after TBI. This novel strategy may aid in exploring the core therapeutic targets for other diseases.

Abbreviations

Cc, candidate compound; CMC-Na, sodium carboxymethyl cellulose; Ct, candidate target; CCI, cortical impact injury; DMSO, dimethyl sulfoxide; DL, drug-likeness; EGFR, epidermal growth factor receptor; GAP43, growth associated protein 43; GFAP, glial fibrillary acidic protein; H&E, Hematoxylin and Eosin; Mp, medicinal plant; O.B, oral bioavailability; PEG, polyethylene glycol; PPI, Protein-protein interaction; SEM, standard error; TCMSP, Traditional Chinese Medicine Systems Pharmacology; TBI, traumatic brain injury.

Funding

This work was supported by the National Natural Science Foundation of China [grant number 82174259, 81973665], The Science and Technology Innovation Program of Hunan Province/the Hunan Provincial Key Research and Development Program [grant number 2023SK2021, 2022SK2015], the Hunan TCM Scientific Research Program [grant number 2021032, D2022065 and B2024113], The National Science Foundation of Hunan Province (2022JJ40853), and the Postdoctoral Fellowship Program of CPSF (GZC20233202).

Disclosure

The authors report no conflicts of interest in this work.

References

1. Maas A, Fitzgerald M, Gao G, et al. Traumatic brain injury over the past 20 years: research and clinical progress. *Lancet Neurol*. 2022;21:768–770. doi:10.1016/S1474-4422(22)00307-6
2. Lee B, Leem J, Kim H, et al. Herbal medicine for acute management and rehabilitation of traumatic brain injury. *Medicine*. 2019;98:e14145. doi:10.1097/MD.0000000000014145
3. Sawmiller D, Li S, Shahaduzzaman M, et al. Luteolin reduces Alzheimer's disease pathologies induced by traumatic brain injury. *Int J Mol Sci*. 2014;15:895–904. doi:10.3390/ijms15010895
4. Wu A, Yong Y, Pan Y, et al. Targeting nrf2-mediated oxidative stress response in traumatic brain injury: therapeutic perspectives of phytochemicals. *Oxid Med Cell Longev*. 2022;2022:1–24. doi:10.1155/2022/3027514
5. Salem M, Shaheen M, Tabbara A, Borjac J. Saffron extract and crocin exert anti-inflammatory and anti-oxidative effects in a repetitive mild traumatic brain injury mouse model. *Sci Rep*. 2022;12:5004. doi:10.1038/s41598-022-09109-9

6. Shi Y, Zhou X, Yang R, Ying S, Wang L. Panax notoginseng protects the rat brain function from traumatic brain injury by inhibiting autophagy via mammalian targeting of rapamycin. *Aging*. 2021;13:11207–11217. doi:10.18632/aging.202790
7. Hu X, Qi C, Feng F, et al. Combining network pharmacology, RNA-seq, and metabolomics strategies to reveal the mechanism of cimicifugae rhizoma - smilax glabra Roxb herb pair for the treatment of psoriasis. *Phytomedicine*. 2022;105:154384. doi:10.1016/j.phymed.2022.154384
8. Jafari M, Wang Y, Amiryousefi A, Tang J. Unsupervised learning and multipartite network models: A promising approach for understanding traditional medicine. *Front Pharmacol*. 2020;11:1319. doi:10.3389/fphar.2020.01319
9. Guo F, Tang X, Zhang W, et al. Exploration of the mechanism of traditional Chinese medicine by AI approach using unsupervised machine learning for cellular functional similarity of compounds in heterogeneous networks, XiaoErFuPi granules as an example. *Pharmacol Res*. 2020;160:105077. doi:10.1016/j.phrs.2020.105077
10. Li T, Zhang W, Hu E, et al. Integrated metabolomics and network pharmacology to reveal the mechanisms of hydroxysafflor yellow A against acute traumatic brain injury. *Comput Struct Biotechl J*. 2021;19:1002–1013. doi:10.1016/j.csbj.2021.01.033
11. Hu E, Li T, Li Z, et al. Metabolomics reveals the effects of hydroxysafflor yellow A on neurogenesis and axon regeneration after experimental traumatic brain injury. *Pharm Biol*. 2023;61:1054–1064. doi:10.1080/13880209.2023.2229379
12. Hu E, Li Z, Li T, et al. A novel microbial and hepatic biotransformation-integrated network pharmacology strategy explores the therapeutic mechanisms of bioactive herbal products in neurological diseases: the effects of astragaloside IV on intracerebral hemorrhage as an example. *Chin Med*. 2023;18:40. doi:10.1186/s13020-023-00745-5
13. Xu J, Wang H, Ding K, et al. Luteolin provides neuroprotection in models of traumatic brain injury via the nrf2–are pathway. *Free Radic Biol Med*. 2014;71:186–195. doi:10.1016/j.freeradbiomed.2014.03.009
14. Chin C, Chen S, Wu H, Ho C, Ko M, Lin C. cytoHubba: identifying hub objects and sub-networks from complex interactome. *BMC Syst Biol*. 2014;8(Suppl 4):S11. doi:10.1186/1752-0509-8-S4-S11
15. Yang Z, Guo Q, Wang Y, et al. Azd3759, a BBB-penetrating EGFR inhibitor for the treatment of EGFR mutant NSCLC with CNS metastases. *Sci Transl Med*. 2016;8:368ra172. doi:10.1126/scitranslmed.aag0976
16. Zhang Y, Sloan SA, Clarke LE, et al. Purification and characterization of progenitor and mature human astrocytes reveals transcriptional and functional differences with mouse. *Neuron*. 2016;89:37–53. doi:10.1016/j.neuron.2015.11.013
17. Mcgovern AJ, Barreto GE. Network pharmacology identifies il6 as an important hub and target of tibolone for drug repurposing in traumatic brain injury. *Biomed Pharmacother*. 2021;140:111769. doi:10.1016/j.biopha.2021.111769
18. Lupo G, Gioia R, Nisi PS, Biagioni S, Cacci E. Molecular mechanisms of neurogenic aging in the adult mouse subventricular zone. *J Exp Neurosci*. 2019;13:1509773112. doi:10.1177/1179069519829040
19. Zhang S, Ju P, Tjandra E, Yeap Y, Owlanj H, Feng Z. Inhibition of epidermal growth factor receptor improves myelination and attenuates tissue damage of spinal cord injury. *Cell Mol Neurobiol*. 2016;36:1169–1178. doi:10.1007/s10571-015-0313-4
20. Goldshmit Y, Schokoroy Trangle S, Afergan F, Iram T, Pinkas-Kramarski R. Nucleolin inhibitor groa triggers reduction in epidermal growth factor receptor activation: pharmacological implication for glial scarring after spinal cord injury. *J Neurochem*. 2016;138:845–858. doi:10.1111/jnc.13730
21. Li Z, Li J, Wang L, et al. Epidermal growth factor receptor inhibitor ameliorates excessive astrogliosis and improves the regeneration microenvironment and functional recovery in adult rats following spinal cord injury. *J Neuroinflam*. 2014;11:71. doi:10.1186/1742-2094-11-71
22. Li Z, Tang R, Zhang J, et al. Inhibiting epidermal growth factor receptor attenuates reactive astrogliosis and improves functional outcome after spinal cord injury in rats. *Neurochem Int*. 2011;58:812–819. doi:10.1016/j.neuint.2011.03.007
23. Okada S, Hara M, Kobayakawa K, Matsumoto Y, Nakashima Y. Astrocyte reactivity and astrogliosis after spinal cord injury. *Neurosci Res*. 2018;126:39–43. doi:10.1016/j.neures.2017.10.004
24. Li H, Pan Y, Sun Z, Sun Y, Yang X, Feng D. Inhibition of mir-21 ameliorates excessive astrocyte activation and promotes axon regeneration following optic nerve crush. *Neuropharmacology*. 2018;137:33–49. doi:10.1016/j.neuropharm.2018.04.028
25. Hara M, Kobayakawa K, Ohkawa Y, et al. Interaction of reactive astrocytes with type I collagen induces astrocytic scar formation through the integrin–n-cadherin pathway after spinal cord injury. *Nat Med*. 2017;23:818–828. doi:10.1038/nm.4354
26. Tavassoly O, Del Cid Pellitero E, Larroquette F, et al. Pharmacological inhibition of brain EGFR activation by a BBB-penetrating inhibitor, AZD3759, attenuates α-synuclein pathology in a mouse model of α-synuclein propagation. *Neurotherapeutics*. 2021;18:979–997. doi:10.1007/s13311-021-01017-6
27. Ahn M, Kim D, Cho BC, et al. Activity and safety of AZD3759 in EGFR-mutant non-small-cell lung cancer with CNS metastases (BLOOM): a phase 1, open-label, dose-escalation and dose-expansion study. *Lancet Respir Med*. 2017;5:891–902. doi:10.1016/S2213-2600(17)30378-8
28. Zeng Q, Wang J, Cheng Z, et al. Discovery and evaluation of clinical candidate azd3759, a potent, oral active, central nervous system-penetrant, epidermal growth factor receptor tyrosine kinase inhibitor. *J Med Chem*. 2015;58:8200–8215. doi:10.1021/acs.jmedchem.5b01073
29. Yin W, Zhang K, Deng Q, et al. Azd3759 inhibits glioma through the blockade of the epidermal growth factor receptor and janus kinase pathways. *Bioengineered*. 2021;12:8679–8689. doi:10.1080/21655979.2021.1991160
30. Chu Q, Wu T, Fu L, Ye J. Simultaneous determination of active ingredients in erigeron breviscapus (vant.) Hand-mazz. By capillary electrophoresis with electrochemical detection. *J Pharm Biomed Anal*. 2005;37:535–541. doi:10.1016/j.jpba.2004.11.018
31. Lee JY, Chang EJ, Kim HJ, Park JH, Choi SW. Antioxidative flavonoids from leaves of carthamus tinctorius. *Arch Pharm Res*. 2002;25:313–319. doi:10.1007/BF02976632
32. Xiong Y, Zhong W, Liu J, et al. Luteolin isolated from Polygonum cuspidatum is a potential compound against nasopharyngeal carcinoma. *Biomed Res Int*. 2022;2022:1–21.
33. Ye B, Chen P, Lin C, Zhang C, Li L. Study on the material basis and action mechanisms of sophora davidii (franch.) skeels flower extract in the treatment of non-small cell lung cancer. *J Ethnopharmacol*. 2023;317:116815. doi:10.1016/j.jep.2023.116815
34. Wu H, Mahmood A, Lu D, et al. Attenuation of astrogliosis and modulation of endothelial growth factor receptor in lipid rafts by simvastatin after traumatic brain injury. *J Neurosurg*. 2010;113:591–597. doi:10.3171/2009.9.JNS09859
35. Zhou Y, Shao A, Yao Y, Tu S, Deng Y, Zhang J. Dual roles of astrocytes in plasticity and reconstruction after traumatic brain injury. *Cell Commun Signal*. 2020;18:62. doi:10.1186/s12964-020-00549-2